Interface transport scheme of a two-phase flow by the method of characteristics

Mireille El-Haddad, Frédéric Hecht, Toni Sayah

INTERFACE TRANSPORT SCHEME OF A TWO-PHASE FLOW BY THE METHOD OF CHARACTERISTICS.

MIREILLE HADDAD[†‡], FRÉDÉRIC HECHT[†], AND TONI SAYAH[‡]

Abstract. In this paper, we study an interface transport scheme of a two-phase flow of an incompressible viscous immiscible fluid. The problem is discretized by the characteristics method in time and finite elements method in space. The interface is captured by the Level-Set function. Appropriate boundary conditions for the problem of mould filling are investigated, a new natural boundary condition under pressure effect for the transport equation is proposed and an algorithm for computing the solution is presented. Finally, numerical experiments show and validate the effectiveness of the proposed scheme.

Keywords. Two-phase flow, Level-Set function, finite element method, characteristics method, boundary condition under pressure effect.

1. Introduction.

This paper is devoted to the study of an interface transport scheme separating two immiscible incompressible viscous fluids. This problem involves a wide range of real-life physical phenomena having a major importance in several industrial applications; within which we are especially interested in modeling mould filling in iron foundry. In many such fluid flows, the physical time scale and length scales are so small that credible experiments are very expensive. Thus numerical analysis appears to be the only way to understand and solve the problem. The development of a reliable computational strategy of such problems requires the accurate discretization and tracking of the free surface.

There are, however, major challenges in the context of multiphase flow modeling. First, we have to take into account the evolution of the interface and its topological changes. Second, we have to deal with the non-linearity for the convection of the flow and the interface. Third, we must assign appropriate boundary conditions to the flow and transport equations. In addition, care must be taken in treating the geometrical and topological singularities across the interface. We also have to maintain a sharp interface resolution, including the cases of interface folding, breaking and merging. Finally, we should respect the physical properties such as the mass conservation for any incompressible fluid flows.

Since the seminal work of Harlow and Welch [22], several methods have been developed to solve the problem of interfacial flows numerically, we cite these studies [1], [13],[39] and the references therein as examples. The most popular way is to divide these methods into two main categories according to the mesh:

(1) In the Lagrangian methods, a set of equidistant markers is used to track the interface motion. Each computational cell carries always the same fluid portion and the mesh moves with the fluid. As time evolves, marker points have to be relocated along the new interface. Furthermore, this method requires the transfer of information between the interface and the fixed mesh once the interface has been moved. In addition, in this approach it is hard to deal with the evolution of interface markers when the interface becomes severely stretched or deformed. More details about

October 20, 2015.

[†] Laboratoire Jacques-Louis Lions, F-75005, Paris, France Sorbonne Université, UPMC Univ Paris 06, UMR 7598, Laboratoire Jacques-Louis Lions, F-75005, Paris, France.

[‡] Unité de recherche EGFEM, Faculté des Sciences, Université Saint-Joseph, B.P 11-514 Riad El Solh, Beyrouth 1107 2050, Liban.

e-mails:elhaddad@ljll.math.upmc.fr, frederic.hecht@upmc.fr, toni.sayah@usj.edu.lb.

these methods and their implementation can be found in the references [49], [20], [21], [24] and [15]. Some attempts to overcome the drawbacks of these methods have been made, hybrid approaches like the arbitrary Lagrangian-Eulerian (ALE) method have been proposed among which we may cite [48], [37], [3], [6] and [18]. They consist in solving the problem using a mesh and then the later is moved according to the flow velocity field. The ALE schemes lead to satisfying results but the intricacy of implementation seems to be expensive, especially in three-dimensional problems.

(2) The Eulerian techniques are characterized by a fixed mesh and the fluid travels from one grid cell to another. The most commonly used approaches among the Eulerian techniques are the interface capturing methods. The location of the interface is determined by the advection of either a characteristic function or a zero-isocontour of a continuous function by the fluid velocity. The obtained transport equation expresses that the interface is a material line propagating with the fluid.
   - The discontinuous approach was introduced by Hirt and Nichols [25] by the so-called volume-of-fluid (VOF) method. This is the first interface capturing method using the concept of transport of a scalar field. The main idea of the VOF method is to use a scalar field to locate the two fluids. It is a very popular method for modeling free boundaries in hydrodynamics problems. The advantages of this tool that it can manage topology changes in the interface like breaks and reconnections, it naturally conserves mass, and it can be easily extended to 3D (see [25] and [35]). The major drawbacks of the method are the necessity to advect a discontinuous function which requires a specific numerical treatment of the transport equation, the difficulties in determining the precise location of the interface as well as its geometric characteristics. Moreover, even if some reconstruction algorithms are effective in improving the precision, they are complex and expensive to implement in 3D. Finally, the quality of this method will depend both of the reconstruction method of interface and of the numerical scheme for solving the transport equation.
   - The first algorithm on the continuous interface capturing approach was suggested by Dervieux and Thomasset [14]. Later, the development of this approach evolved based on the Level-Set method, we may cite [31], [42], [9], [50], [51] and [43]. The concept of this method is to define a regular scalar function through the interface (distance function), whose zero level set is the interface that we are looking to describe. Solving the transport equation by advecting this distance function makes it possible to predict the evolution of the interface propagating with the fluid velocity field. The Level-Set method takes into account the topological changes naturally. It simplify considerably the interface convection problem (as far as convecting a continuous function is much easier than convecting a discontinuous one). It also makes it easy to compute the geometric characteristics from the distance function and it is easy to be extended to 3 dimensional problems. However, a number of disadvantages can affect the performance of the method. During the computing process after many time steps, the distance property and the mass are not preserved. A reinitialization algorithm is usually used to keep the level set function a signed distance function and a mass conservation process is required in order to respect the physical properties.

Based on this state of art, we are motivated to select the context of the Level-Set method. Also, we decouple the purely convective part of the flow and of the transport equation from the advection part; the treatment of the nonlinear convection term is thus reduced to a problem of research of characteristic curves. Furthermore, we select the finite element scheme for the spacial discretization and we maintain the convenience and effectiveness of Eulerian grid. In addition, we choose the Galerkin finite element for the discretization in space as it assumes the minimal regularity for the existence and the uniqueness of a solution.

The outline of the paper is as follows:

- In section 2, we present the problem of mould filling.
- In section 3, we analyze the corresponding continuous problem.

- In section 4, we introduce the discrete problem and recall its main properties.
- In section 5, we study the problem by the projection method.
- In section 6, we correct the Level set by reinitialisation and mass conservation.
- In section 7, we show numerical results of validation.

2. Problem of mould filling

To formulate the appropriate mathematical model to our problem, we start by the physical hypothesis that we have assumed. We consider an unsteady and laminar flow of two immiscible fluids. In this flow, the two fluids are supposed to be viscous, Newtonian and of large density ratio. In addition, the fluids are considered incompressible and isothermal, thus neglecting the variations of density and viscosity due to changes in pressure or temperature. Furthermore, by assuming that both fluids are homogenous, we believe that the viscosity and density are constants in each fluid. The two fluids are immiscible and the separation zone between the fluids is a sharp interface of zero thickness wherein the physical properties of the two fluids change abruptly. To treat the variations of the physical properties across the interface, it is necessary to implement jump conditions. In our study, we neglect the surface tension between the two fluids. We assume the interface is impermeable, thus the mass transfer across the interface is neglected (See [4] and [26]).

We consider an interval $[0,T] \subset \mathbb{R}$, where T is a positive real number, and an arbitrary time $t \in [0,T]$. Let Ω be a bounded simply connected open domain in $\mathbb{R}^d$, $d = 2, 3$, with a Lipschitz-continuous connected boundary $\partial\Omega$. We denote by $\mathbf{n}$ the outward unit normal vector to the interface $\partial\Omega$ and $(\mathbf{e_1}, \mathbf{e_2})$ the canonical base of $\mathbb{R}^2$ (respectively $(\mathbf{e_1}, \mathbf{e_2}, \mathbf{e_3})$ the canonical base of $\mathbb{R}^3$).

We suppose that Ω represents a mould containing two fluids, thus, at each time $t \in [0,T]$, it is divided into two open sub-domains Ω_1 and Ω_2 evolving in time and separated by the interface Γ such that $\overline{\Omega} = \overline{\Omega}_2(t) \cup \overline{\Omega}_2$ and $\Omega_1(t) \cap \Omega_2(t) = \emptyset$.

We denote by $\partial\Omega_i$ the boundary Ω_i, $i = 1, 2$, which is divided into four parts such that $\partial\Omega_1 \cap \partial\Omega_2 = \Gamma(t)$, $\partial\Omega = \Gamma_0 \cup \Gamma_1 \cup \Gamma_2$ where Γ_0 is the bottom of the boundary as indicated in figure 1 (corresponding to the inlet), Γ_2 is the top of the boundary (corresponding to the free boundary of the fluid) and $\Gamma_1 = \partial\Omega \setminus (\Gamma(t) \cup \Gamma_0 \cup \Gamma_2)$ (corresponding to the wall).

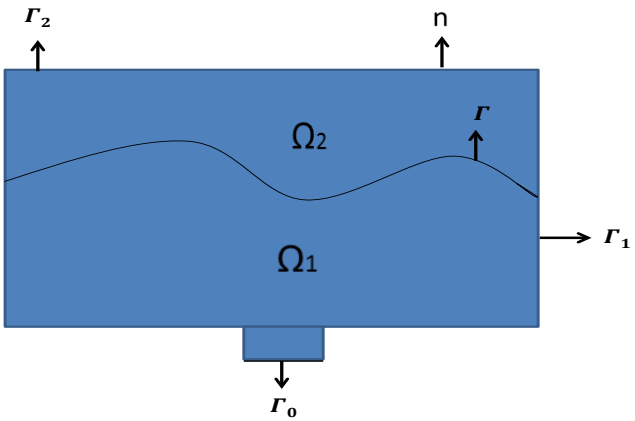

Figure 1. An arbitrary domain Ω

We denote by $\mathbf{u}^i$ and p^i respectively the velocity and the pressure in the domain $\Omega^i, i = 1, 2$, and by μ^i and ρ^i respectively the constant dynamic viscosities and densities of the fluid in $\Omega^i, i = 1, 2$.
The bi-fluid flow motion is described in each subdomain and at each time $t \in]0,T[$ by the following

incompressible Navier-Stokes equations.

$$\begin{cases} \rho^i\Big(\dfrac{\partial \mathbf{u}^i}{\partial t} + (\mathbf{u}^i.\nabla)\mathbf{u}^i\Big) - \operatorname{div}(2\mu^i\ \mathbb{D}\mathbf{u}^i) + \nabla p^i = \mathbf{f}^i & \text{in} \quad \Omega^i\ (i=1,2), \\ \operatorname{div}\ \mathbf{u}^i = 0 & \text{in} \quad \Omega^i\ (i=1,2), \end{cases} \tag{2.1}$$

where $\mathbb{D}\mathbf{u}^i = \dfrac{1}{2}(\nabla \mathbf{u}^i + {}^t\nabla \mathbf{u}^i)$ is the deformation rate tensor and f^i represents a density of body forces in $\Omega^i, i = 1, 2$.

The density (respectively the viscosity) of the fluid can be written in Ω as

$$\rho(\mathbf{x},t) = \rho_1 1_{\mathbf{x}\in\Omega_1(t)} + \rho_2 1_{\mathbf{x}\in\Omega_2(t)} \ \ (\text{respectively } \mu(\mathbf{x},t) = \mu_1 1_{\mathbf{x}\in\Omega_1(t)} + \mu_2 1_{\mathbf{x}\in\Omega_2(t)}),$$

where $1_{\mathbf{x}\in\Omega_i}$ is the characteristic function of the subdomain $\Omega_i, i = 1, 2$.
We denote by $\mathbf{f}$ the data, $\mathbf{u}$ the velocity and p the pressure of the fluid in Ω such that $\mathbf{f} = \mathbf{f}_i$, $\mathbf{u} = \mathbf{u}_i$ and $p = p_i$ in $\Omega^i, i = 1, 2$. The problem (2.1) can be rewritten as: at each time $t \in]0, T[$

$$\begin{cases} \rho\Big(\dfrac{\partial \mathbf{u}}{\partial t} + (\mathbf{u}.\nabla)\mathbf{u}\Big) - \operatorname{div}(2\mu\ \mathbb{D}\mathbf{u}) + \nabla p = \mathbf{f} & \text{in} \quad \Omega_1 \cup \Omega_2\ , \\ \operatorname{div}\ \mathbf{u} = 0 & \text{in} \quad \Omega_1 \cup \Omega_2. \end{cases} \tag{2.2}$$

This system must be endowed with adequate boundary and initial conditions, thus, we will consider on the inlet Γ_0 a non-homogeneous boundary condition of Dirichlet type: $\mathbf{u} = U_{in}$, on the free surface Γ_2 a do nothing boundary condition: $(2\mu\mathbb{D}\mathbf{u} - pI).\mathbf{n} = 0$ and on the wall Γ_1 we will compare two different boundary conditions:

$$(BCU)\begin{cases} \text{Dirichlet boundary conditions:} & \mathbf{u} = 0 \\ \text{or} & \\ \text{Navier boundary conditions:} & \mathbf{u}.\mathbf{n} = 0 \\ & \text{and} \quad \alpha\mathbf{u}.\boldsymbol{\tau} + {}^t\mathbf{n}(2\mu\mathbb{D}\mathbf{u} - pI).\boldsymbol{\tau} = 0, \end{cases}$$

where $\boldsymbol{\tau}$ is the tangential unit vector and α is the friction coefficient.
In fact, a lot of works consider boundary conditions of Dirichlet type. However, as noted by Serrin [36], they are not always realistic and in general lead to boundary layers phenomena next to the walls (As we will see in the numerical results). Navier [28] has proposed a so-called slip boundary provided with friction at the wall which allows taking into account the slip of fluid next to the boundaries and measure the friction effect.

Besides, the system (2.2) is also completed with interface conditions imposing the continuity of the velocity and the balance of the normal stress with the surface tension across the interface $\Gamma(t)$, namely:

$$[\mathbf{u}]|_\Gamma = 0 \text{ and } [2\mu\mathbb{D}\mathbf{u} - pI]|_\Gamma.\mathbf{n} = 0,$$

where $[.]|_\Gamma$ denotes the jump of quality across Γ in the normal direction of Ω_1, i.e. $[.]|_\Gamma = .|_{\Omega_1} - .|_{\Omega_2}$.
In this paper, we neglected the surface tension.

We intend to work with the following problem: at each time $t \in]0,T[$,

$$\begin{cases} \rho\Big(\dfrac{\partial \mathbf{u}}{\partial t} + (\mathbf{u}.\nabla)\mathbf{u}\Big) - \operatorname{div}(2\mu\mathbb{D}\mathbf{u}) + \nabla p = \mathbf{f} & \text{in} \quad \Omega_1 \cup \Omega_2\ , \\ \operatorname{div}\mathbf{u} = 0 & \text{in} \quad \Omega, \\ \mathbf{u} = U_{in} & \text{on} \quad \Gamma_0, \\ (BCU) & \text{on} \quad \Gamma_1, \\ (2\mu\mathbb{D}\mathbf{u} - pI).\mathbf{n} = 0 & \text{on} \quad \Gamma_2, \\ [2\mu\mathbb{D}\mathbf{u} - pI].\mathbf{n} = 0 & \text{on} \quad \Gamma, \\ [\mathbf{u}] = 0 & \text{on} \quad \Gamma, \\ \mathbf{u}(\mathbf{x},0) = 0 & \text{in} \quad \Omega, \end{cases} \tag{2.3}$$

where $\mathbf{f} = -\rho g \mathbf{e_d}$ is the gravitational force vector, I is the identity matrix and U_{in} designates the velocity of the flux at the inlet.

For the interface transport, the main challenge is to handle geometrical and topological changes. Thus we solve the problem using the level set function on a fixed uniform mesh. In particular, we follow here Osher and Sethian (see [31]), we introduce the signed distance function to the interface $\Gamma(t)$:

$$\phi(x,t) = \pm \min_{y \in \Gamma(t)} |x - y|, \tag{2.4}$$

where the function ϕ is set to be negative in the domain $\Omega_1(t)$ and positive in the domain $\Omega_2(t)$. Hence, at each time step, the fluid interface corresponds to the zero isocontours of the continuous function ϕ:

$$\Gamma = \{\mathbf{x} \in \mathbb{R}^d / \phi(\mathbf{x},t) = 0,\ \forall t \geq 0\}.$$

The density ρ and the viscosity μ can be rewritten in Ω as:

$$\rho(\mathbf{x},t) = \rho_1(\phi \leq 0) + \rho_2(\phi > 0) \text{ and } \mu(\mathbf{x},t) = \mu_1(\phi \leq 0) + \mu_2(\phi > 0).$$

The interface is then captured, at each time step, by the advection of the Level set function by the fluid velocity. It can be described by the following transport equation:

$$\frac{\partial \phi}{\partial t} + \mathbf{u}.\nabla\phi = 0. \tag{2.5}$$

After a very small time, discontinuities appear over the interface next to the boundaries because there is no uniqueness of the solution for a general continuous velocity field $\mathbf{u}$ in this strong formulation. To avoid them we may find the solution in the sense of viscosity. This method was introduced by P.L.Lions et M.G. Crandall [12] and selects the weak discontinuous physically significant solution by adding an artificial viscosity $-\varepsilon\Delta\phi$ that vanishes as $\varepsilon \to 0$ [5].

We denote by h the grid size of the mesh, we choose the parameter ε to be proportional to h as in [29]. The choice of ε is very delicate, a small ε gives better conservation of the area (volume) bounded by the zero contour of ϕ since the volume error increases proportionally to ε. There are however numerical restrictions on how small we can choose this parameter [30]. In our application, numerical tests showed that below a critical value of epsilon (for $\varepsilon \leq h/50$) discontinuities occur over the interface, for $h/50 \leq \varepsilon < h/3$ oscillations occur over the interface and for $\varepsilon \geq h/3$ we obtain neither discontinuities nor oscillations but the volume error is remarkably large (as we will show in the numerical results).

Appropriate boundary and initial condition must also be assigned to ϕ. There exists in the literature variant of boundary conditions that can be assigned to ϕ, for example Dirichlet boundary condition, homogeneous Neumann boundary condition and contact line boundary condition which depends on the

wettability property of a solid surface by a liquid via the Young equation [34]),...

In this work, we will consider homogeneous Neumann boundary condition which are used in a lot of applications (See for example [29]) and we will propose a new natural boundary condition which will be called non-homogeneous boundary condition under pressure effect. This last one calculates the slope of the angle between the free surface and the wall boundaries in a natural way that makes sense from physical point of view. The non-homogeneous boundary condition on Γ_1 under pressure effect is a boundary condition on the pressure:
We multiply the first equation of (2.3) by $\mathbf{n}$.

$$\rho\partial_t\mathbf{u}.\mathbf{n}|_{\Gamma_1} + \rho\Big((\mathbf{u}.\nabla)\mathbf{u}\Big).\mathbf{n}|_{\Gamma_1} - \mathrm{div}(2\mu\mathbb{D}\mathbf{u}).\mathbf{n}|_{\Gamma_1} + \nabla p.\mathbf{n}|_{\Gamma_1} = -\rho g\mathbf{e_d}.\mathbf{n}|_{\Gamma_1} \tag{2.6}$$

The first term $(\partial_t\mathbf{u}).\mathbf{n} = \partial_t(\mathbf{u}.\mathbf{n}) = 0$ since $\mathbf{u}.\mathbf{n} = 0$.

And we get the following boundary condition on Γ_1:

$$\partial_{\mathbf{n}}p|_{\Gamma_1} = -\rho g\mathbf{e_d}.\mathbf{n}|_{\Gamma_1} - \rho\Big((\mathbf{u}.\nabla)\mathbf{u}\Big).\mathbf{n}|_{\Gamma_1} - 2\mu\mathbb{D}\mathbf{u}.\mathbf{n}|_{\Gamma_1}.$$

In our application, the viscosity is a very small number. Thus we neglect the second term in the right hand side of the last equation and the boundary condition on the pressure on Γ_1 can be written as:

$$\partial_{\mathbf{n}}p|_{\Gamma_1} = -\rho g\mathbf{e_d}.\mathbf{n}|_{\Gamma_1} - \rho\Big((\mathbf{u}.\nabla)\mathbf{u}\Big).\mathbf{n}|_{\Gamma_1}.$$

We neglect the pressure of gravity in Ω_2 which contain a fluid with very small density, then the pressure vanishes on the interface which is the zero isocontour. Hence the pressure and the Level-Set function have the same isovalues $\phi = p = 0$ on the free surface which implies that ϕ can be considered as equal to p up to a multiplicative constant c ($\phi = -cp$) in a neighborhood of the boundary Γ.

The non-homogeneous boundary condition under pressure effect can be written on Γ_1 as:

$$\partial_{\mathbf{n}}\phi = -c\partial_{\mathbf{n}}p. \tag{2.7}$$

Since $\|\nabla\phi\| = 1$, we normalize the boundary condition and we get:

$$\partial_{\mathbf{n}}\phi = \frac{\Big(\rho g\mathbf{e_d} + \rho\big((\mathbf{u}.\nabla)\mathbf{u}\big)\Big).\mathbf{n}}{\|\Big(\rho g\mathbf{e_d} + \rho\big((\mathbf{u}.\nabla)\mathbf{u}\big)\Big).\mathbf{n}\|}. \tag{2.8}$$

We denote by $G(u)$ the right hand side of (2.8).
We impose two different boundary conditions on the transport equation on Γ_1:

$$(BC\phi)\begin{cases} \text{Homogeneous Neumann boundary conditions } \ \partial_{\mathbf{n}}\phi = 0 \\ \text{and} \\ \text{Non-homogeneous Neumann boundary conditions under pressure effect } \partial_{\mathbf{n}}\phi = G(\mathbf{u}). \end{cases} \tag{2.9}$$

We will show in the numerical results that these boundary conditions under pressure effects give the physical slope of the angle between the free surface and the interface as well as they decrease remarkably the volume error.
The equation (2.5) endowed with boundary conditions will be written in the following form:

$$\begin{cases} \partial_t\phi + \mathbf{u}.\nabla\phi - \varepsilon\Delta\phi = 0 & \text{in} \quad \Omega, \\ (BC\phi) & \text{on} \quad \Gamma_1, \\ \partial_{\mathbf{n}}\phi = 0 & \text{on} \quad \Gamma_0 \cup \Gamma_2, \\ \phi(\mathbf{x}, 0) = \phi_0 & \text{in} \quad \Omega, \end{cases} \tag{2.10}$$

where ϕ_0 is the initial position of the interface.
Our coupled system of equations will be (2.3) and (2.10). Well-posedness results for the general weak

formulation of the Navier-Stokes problem for two-phase flows including the interface jump condition have been analyzed only for special cases. The case of a bounded domain Ω for arbitrary time intervals $[0,T], T>0$ is treated in [44]; it provides a well-posedness result for the Navier-Stokes problem in a weak formulation.

3. Analysis of the model

In order to write the variational formulation of the previous problem, we introduce the following Sobolev spaces (m and $p \in \mathbb{N}$):

$$W^{m,p}(\Omega) = \{\mathbf{v} \in L^p(\Omega), \partial^\alpha \mathbf{v} \in L^p(\Omega), \forall |\alpha| \leq m\},$$

$$H^m(\Omega) = W^{m,2}(\Omega),$$

equipped with the following semi-norm and norm:

$$|\mathbf{v}|_{m,p,\Omega} = \{ \sum_{|\alpha|=m} \int_\Omega |\partial^\alpha \mathbf{v}(x)|^p dx\}^{\frac{1}{p}}$$

and

$$\|\mathbf{v}\|_{m,p,\Omega} = \{ \sum_{K \leq m} |\mathbf{v}|^p_{k,p,\Omega}\}^{\frac{1}{p}}.$$

We denote by X_u the sub-space of $H^1(\Omega)$ defined by:

$$X_u = \begin{cases} \{\mathbf{u} \in H^1(\Omega) \ / \ \mathbf{u} = U_{in} \ \text{ on } \Gamma_0 \ \textit{and} \ \mathbf{u} = 0 \ \text{ on } \Gamma_1\} & : \ \text{in the case of Dirichlet ,} \\ \{\mathbf{u} \in H^1(\Omega) \ / \ \mathbf{u} = U_{in} \ \text{ on } \Gamma_0\} & : \ \text{in the case of Navier .} \end{cases} \tag{3.1}$$

X_v the sub-space of $H^1(\Omega)$ defined by:

$$X_v = \begin{cases} \{\mathbf{v} \in H^1(\Omega) \ / \ \mathbf{v} = 0 \ \text{ on } \Gamma_0 \cup \Gamma_1 \ \} & : \ \text{In the case of Dirichlet ,} \\ \{\mathbf{v} \in H^1(\Omega) \ / \ \mathbf{v} = \ 0 \quad \text{on } \Gamma_0\} & : \ \text{In the case of Navier .} \end{cases} \tag{3.2}$$

Let $L^2_0(\Omega)$ be the sub-space of L^2 defined by:

$$L^2_0(\Omega) = \{p \in L^2(\Omega) \ / \ \int_\Omega p(x)dx = 0\}.$$

We denote by $M = L^2_0(\Omega)$, $Y = L^2(\Omega)$ and we suppose that $\mathbf{f} \in L^2(\Omega)^d$.
The existence and uniqueness of the solution of the problem of the Navier-Stokes is guaranteed due to the condition of Babuska-Brezzi [17], also called inf-sup condition.

The weak formulation of the problem with the Dirichlet boundary conditions can be written as:
Find $(\mathbf{u}, p) \in X_u \times M$, $\phi \in Y$ such that:

$$\begin{cases} \Big(\dfrac{\partial \phi}{\partial t} + \mathbf{u}.\nabla\phi, r\Big) + \varepsilon(\nabla\phi, \nabla r) - \varepsilon \displaystyle\int_{\Gamma_1} G(\mathbf{u}) r = 0 & \forall \phi \in Y, \\ \rho\Big(\dfrac{\partial \mathbf{u}}{\partial t} + (\mathbf{u}.\nabla)\mathbf{u}, \mathbf{v}\Big) + 2\mu(\mathbb{D}\mathbf{u}, \mathbb{D}\mathbf{v}) - (p, \operatorname{div}\mathbf{v}) = -(\rho g \boldsymbol{e}_d, \mathbf{v}) & \forall \mathbf{v} \in X_v, \\ (q, \operatorname{div}\mathbf{u}) = 0 & \forall q \in M. \end{cases} \tag{3.3}$$

Let us now write the weak formulation with the Navier boundary conditions (BCU). To implement them, we couple the velocity componants in one equation and we use the penalty method as follows:

$$\begin{cases} & \beta^{-1}\mathbf{u}.\mathbf{n} + \ {}^t\mathbf{n}(2\mu\mathbb{D}\mathbf{u} - pI).\mathbf{n} = 0 \\ \text{and} \quad & \alpha\mathbf{u}.\boldsymbol{\tau} + \ {}^t\mathbf{n}(2\mu\mathbb{D}\mathbf{u} - pI).\boldsymbol{\tau} = 0. \end{cases} \tag{3.4}$$

where β is a penalty coefficient which is a small number [2].

Thanks to the condition of incompressibility, it follows the relation $\Delta \mathbf{u} = 2 \operatorname{div} \mathbb{D}\mathbf{u}$. The symmetry of the deformation tensor yields:

$$\begin{aligned}(\mathbb{D}\mathbf{u}, \mathbb{D}\mathbf{v}) &= (\mathbb{D}\mathbf{u}, \frac{\nabla \mathbf{v}}{2}) + (\mathbb{D}\mathbf{u}, \frac{{}^t\nabla \mathbf{v}}{2}) \\ &= (\mathbb{D}\mathbf{u}, \frac{\nabla \mathbf{v}}{2}) + ({}^t\mathbb{D}\mathbf{u}, \frac{{}^t\nabla \mathbf{v}}{2}) \\ &= (\mathbb{D}\mathbf{u}, \nabla \mathbf{v})\end{aligned}$$

and

$$\operatorname{div} 2\mathbb{D}\mathbf{u} = \operatorname{div} \nabla \mathbf{u} + \operatorname{div}({}^t\nabla \mathbf{u}) = \operatorname{div} \nabla \mathbf{u} + \nabla(\operatorname{div} \mathbf{u}) = \operatorname{div}(\nabla \mathbf{u}).$$

Than the weak formulation of the problem with Navier boundary conditions can then be written as:
Find $(\mathbf{u}, p) \in X_u \times M$, $\phi \in Y$ such that:

$$\begin{cases} \Big(\dfrac{\partial \phi}{\partial t} + \mathbf{u}.\nabla\phi, r\Big) + \varepsilon(\nabla\phi, \nabla r) - \varepsilon \displaystyle\int_{\Gamma_1} G(\mathbf{u}) r = 0 & \forall \phi \in Y, \\ \rho\Big(\dfrac{\partial \mathbf{u}}{\partial t} + (\mathbf{u}.\nabla)\mathbf{u}, \mathbf{v}\Big) + \mu(\nabla \mathbf{u}, \nabla \mathbf{v}) - (p, \operatorname{div} \mathbf{v}) & \\ \qquad - \displaystyle\int_{\Gamma_1} \Big(2\mu\, \mathbb{D}\mathbf{u} - pI\Big)\mathbf{n}\ .\mathbf{v}\ ds = -(\rho g \boldsymbol{e}_d, \mathbf{v}) & \forall \mathbf{v} \in X_v, \\ (q, \operatorname{div} \mathbf{u}) = 0 & \forall q \in M. \end{cases} \tag{3.5}$$

The integral over the boundary Γ_1 in (3.5) can be rewritten by decomposing the test function $\mathbf{v}$ in the following way:

$$\mathbf{v} = (\mathbf{v}.\mathbf{n})\mathbf{n} + (\mathbf{v}.\boldsymbol{\tau})\boldsymbol{\tau}.$$

That implies by using the definition of Navier boundary condition (3.4):

$$\begin{aligned}\int_{\Gamma_1} (2\mu\mathbb{D}\mathbf{u} - pI)\mathbf{n}\ .\mathbf{v}\ ds &= \int_{\Gamma_1} {}^t\mathbf{n}(2\mu\mathbb{D}\mathbf{u} - pI)\mathbf{n}\ \mathbf{v}\ .\mathbf{n}\ ds + \int_{\Gamma_1} {}^t\mathbf{n}(2\mu\mathbb{D}\mathbf{u} - pI)\boldsymbol{\tau}\ \mathbf{v}\ .\boldsymbol{\tau} ds \\ &= \int_{\Gamma_1} \beta^{-1}(\mathbf{u}.\mathbf{n})(\mathbf{v}.\mathbf{n}) ds + \int_{\Gamma_1} \alpha(\mathbf{u}.\boldsymbol{\tau})(\mathbf{v}.\boldsymbol{\tau}) ds \\ &= \int_{\Gamma_1} \beta^{-1}\, {}^t\mathbf{u}(\mathbf{n}\ {}^t\mathbf{n})\mathbf{v} ds + \int_{\Gamma_1} \alpha\, {}^t\mathbf{u}(\tau\ {}^t\tau)\mathbf{v} ds,\end{aligned} \tag{3.6}$$

Then, the variational formulation can be written as:
Find $(\mathbf{u}, p) \in X_u \times M$, $\phi \in Y$ such that for all $(\mathbf{v}, q) \in X_v \times M$ and $\forall r \in Y$

$$\begin{cases} \Big(\dfrac{\partial \phi}{\partial t} + \mathbf{u}.\nabla\phi, r\Big) + \varepsilon(\nabla\phi, \nabla r) - \varepsilon \displaystyle\int_{\Gamma_1} G(\mathbf{u}) r = 0. \\ \rho\Big(\dfrac{\partial \mathbf{u}}{\partial t} + (\mathbf{u}.\nabla)\mathbf{u}, \mathbf{v}\Big) + \mu(\nabla \mathbf{u}, \nabla \mathbf{v}) - (p, \operatorname{div} \mathbf{v}) \\ \qquad - \displaystyle\int_{\Gamma_1} \beta^{-1}\, {}^t\mathbf{u}(\mathbf{n}\ {}^t\mathbf{n})\mathbf{v} ds - \int_{\Gamma_1} \alpha\, {}^t\mathbf{u}(\boldsymbol{\tau}\ {}^t\boldsymbol{\tau})\mathbf{v} ds = (-\rho g \mathbf{e}_{\mathbf{d}}, \mathbf{v}). \\ (\operatorname{div} \mathbf{u}, q) = 0. \end{cases} \tag{3.7}$$

4. The discrete problem

In this section, we present the numerical strategy we have designed to resolve the continuous coupled system obtained in the previous section. Our approach is based on the characteristics method combined with a finite element method.

4.1. **Discretization in time.** We propose a time discretization of (3.5) and (3.7) by the method of characteristics. This method, also known as the Lagrange-Garlekin method was introduced by Benqué [8] and analyzed in [33]. The main idea behind this method is that the convection operator (the non linear term) can be turned into a total derivative by using a Lagrangian formulation. Thus, the treatment of the nonlinear convection term is reduced to a problem of searching the characteristic foot $X(\mathbf{x}; s; t)$, i.e the position of the particle at the previous time. This approach allows us to avoid theoretically the constraint CFL (Courant-Friedrichs-Levy) on the time step and it has been shown that it has very good stability properties, we may cite [33], [27] and [16]. Furthermore, only the right-hand side has to be updated at each iteration during the resolution.
Thanks to this formulation, it is theoretically possible to follow the particles over time along their trajectory by solving, for each particle, an ordinary differential equation called characteristics equation:

$$\begin{cases} \dfrac{\partial X}{\partial t}(\mathbf{x}, s; t) = \mathbf{u}(X(\mathbf{x}, s; t), t), \\ X(\mathbf{x}, s; s) = x, \end{cases} \tag{4.1}$$

where the characteristics curve $X(\mathbf{x}, s; t)$ denotes the position at time t of a fluid particle located at position $\mathbf{x}$ at the time s.

We introduce a partition of the interval $[0, T]$ into N subintervals $[t_n, t_{n+1}]$, such that $\Delta t = \dfrac{T}{N}$, the points $t_n = n\Delta t$, for $n = 0, ..., N$, and denote by $\mathbf{u}^n(x) = \mathbf{u}(x, t^n)$, $p^n(x) = p(x, t^n)$,$\rho^n(x) = \rho(x, t^n)$, $\mu^n(x) = \mu(x, t^n)$ and $\phi^n(x) = \phi(x, t^n)$.

Using the following approximation of the total derivative along the characteristic curves, we approximate $\dfrac{D\mathbf{u}}{Dt}$ at the time $t = t^{n+1}$ by:

$$\frac{D\mathbf{u}}{Dt}^{n+1} \approx \frac{\mathbf{u}(x, t^{n+1}) - \mathbf{u}(X^n(x), t^n)}{\Delta t}, \tag{4.2}$$

where $X^n(x)$ is the approximation of $X(x, t^{n+1} : t^n)$.
Same for $\dfrac{D\phi}{Dt}$ we approximate it at the time $t = t^{n+1}$ by:

$$\frac{D\phi}{Dt}^{n+1} \approx \frac{\phi(x, t^{n+1}) - \phi(X^n(x), t^n)}{\Delta t}. \tag{4.3}$$

Then along the characteristic curves, the variational formulation with Dirichlet boundary conditions becomes:

$$\begin{cases} \Big(\dfrac{\phi^{n+1} - \phi^n oX^n}{\Delta t}, r\Big) + (\varepsilon\nabla\phi^{n+1}, \nabla r) - \varepsilon\displaystyle\int_{\Gamma_1} G(\mathbf{u}^n)r = 0 & \forall r \in Y, \\ \rho^n\Big(\dfrac{\mathbf{u}^{n+1} - \mathbf{u}^n oX^n}{\Delta t}, \mathbf{v}\Big) + \mu^n\ (\nabla\mathbf{u}^{n+1}, \nabla\mathbf{v}) - (p^{n+1}, \operatorname{div}\mathbf{v}) = (-\rho^n g\mathbf{e_d}, \mathbf{v}) & \forall \mathbf{v} \in X_v, \\ (q, \operatorname{div}\mathbf{u^{n+1}}) = 0 & \forall q \in M, \end{cases} \tag{4.4}$$

and the variational formulation with Navier boundary conditions becomes:

$$\begin{cases} \Big(\dfrac{\phi^{n+1} - \phi^n oX^n}{\Delta t}, r\Big) + (\varepsilon\nabla\phi^{n+1}, \nabla r) - \varepsilon\displaystyle\int_{\Gamma_1} G(\mathbf{u}^n)r = 0 & \forall r \in Y, \\ \rho^n\Big(\dfrac{\mathbf{u}^{n+1} - \mathbf{u}^n oX^n}{\Delta t}, \mathbf{v}\Big) + \mu^n\ (\nabla\mathbf{u}^{n+1}, \nabla\mathbf{v}) - (p^{n+1}, \operatorname{div}\mathbf{v}) \\ -\displaystyle\int_{\Gamma_1} \alpha\ {}^t\mathbf{u}^{n+1}(\boldsymbol{\tau}\ \ {}^t\boldsymbol{\tau})\mathbf{v}ds - \int_{\Gamma_1} \beta^{-1}\ {}^t\mathbf{u}^{n+1}(\mathbf{n}\ \ {}^t\mathbf{n})\mathbf{v}ds = (-\rho^n g\mathbf{e_d}, \mathbf{v}) & \forall \mathbf{v} \in X_v, \\ (q, \operatorname{div}\mathbf{u^{n+1}}) = 0 & \forall q \in M. \end{cases} \tag{4.5}$$

4.2. **Discretization in space.** Let τ_h be a regular family of triangulations of Ω by triangles of tetrahedron k, of parameter h.

We introduce the discrete spaces $X_{u,h} \subset X_u$, $X_{v,h} \subset X_v$, $M_h \subset M$, $Y_h \subset Y$ and we denote by $\mathbf{u}_h^{n+1}$, p_h^{n+1} et ϕ_h^{n+1} respectively the discrete velocity, pressure and Level-Set function.

The velocity is discretized with the Mini-Element:

$$X_{u,h} = \{\mathbf{u}_h \in X_u; \forall k \in \tau_h; \mathbf{u}_{h|k} \in P_b(k)^d\}$$

and

$$X_{v,h} = \{\mathbf{v}_h \in X_v; \forall k \in \tau_h; \mathbf{v}_{h|k} \in P_b(k)^d\},$$

where the space $P_b(k)$ is spanned by functions in $P_1(k)$ and the bubble function on k (for each element k, the bubble function is equal to the product of the barycentric coordinates associated with the vertices of k).

The pressure is discretized with classical continuous finite element of order one:

$$M_h = \{q_h \in M \cap C^0(\Omega); \forall k \in \tau_h, q_{h|k} \in P_1(k)\}.$$

The Level-Set function is also discretized with classical continuous finite element of order one:

$$Y_h = \{r_h \in Y \cap C^0(\Omega); \forall k \in \tau_h, r_{h|k} \in P_1(k)\}.$$

The discrete system corresponding to the variational formulation with Dirichlet boundary conditions can be written in the following form:
Find $(\mathbf{u}_h^{n+1}, p_h^{n+1}) \in X_{u,h} \times M_h$ and $\phi_h \in Y_h$ such that

$$\begin{cases} \Big(\dfrac{\phi_h^{n+1} - \phi_h^n oX^n}{\Delta t}, r_h\Big) + (\varepsilon \nabla \phi_h^{n+1}, \nabla r_h) - \varepsilon \displaystyle\int_{\Gamma_1} G(\mathbf{u}_h^n) r_h = 0 & \forall r_h \in Y_h, \\ \rho_h^n \Big(\dfrac{\mathbf{u}_h^{n+1} - \mathbf{u}_h^n oX^n}{\Delta t}, \mathbf{v}_h\Big) + \mu_h^n \ (\nabla \mathbf{u}_h^{n+1}, \nabla \mathbf{v}_h) - (p_h^{n+1}, \operatorname{div} \mathbf{v}_h) = (f^n, \mathbf{v}_h) & \forall \mathbf{v}_h \in X_{v,h}, \\ (q_h^{n+1}, \operatorname{div} \mathbf{u}_h^{n+1}) = 0 & \forall q_h \in M_h, \end{cases} \tag{4.6}$$

where ρ_h^n et μ_h^n are the corresponding discrete densities and viscosities.

The discrete system corresponding to the variational formulation with Navier boundary conditions can be written in the following form:
Find $(\mathbf{u}_h^{n+1}, p_h^{n+1}) \in X_{u,h} \times M_h$ and $\phi_h \in Y_h$ such that

$$\begin{cases} \Big(\dfrac{\phi_h^{n+1} - \phi_h^n oX^n}{\Delta t}, r_h\Big) + (\varepsilon \nabla \phi_h^{n+1}, \nabla r_h) - \varepsilon \displaystyle\int_{\Gamma_1} G(\mathbf{u}_h^n) r_h = 0 & \forall r_h \in Y_h, \\ \rho_h^n \Big(\dfrac{\mathbf{u}_h^{n+1} - \mathbf{u}_h^n oX^n}{\Delta t}, \mathbf{v}_h\Big) + \mu_h^n \ (\nabla \mathbf{u}_h^{n+1}, \nabla \mathbf{v}_h) - (p_h^{n+1}, \operatorname{div} \mathbf{v}_h) \\ - \displaystyle\int_{\Gamma_1} \alpha \ {}^t\mathbf{u}_h^{n+1} (\boldsymbol{\tau} \ {}^t\boldsymbol{\tau}) \mathbf{v}_h ds - \int_{\Gamma_1} \beta^{-1} \ {}^t\mathbf{u}_h^{n+1} (\mathbf{n} \ {}^t\mathbf{n}) \mathbf{v}_h ds = (-\rho_h^n g \mathbf{e_d}, \mathbf{v}_h) & \forall \mathbf{v} \in X_v, \\ (q_h, \operatorname{div} \mathbf{u_h^{n+1}}) = 0 & \forall q_h \in M_h. \end{cases} \tag{4.7}$$

In the following, we call the schemes (4.6) and (4.7) by the "classical method" for corresponding Dirichlet and Navier boundary conditions.

5. Projection method

In this section, in order to reduce the CPU time and the used memory for the simulation of the problem, we use the projection method to solve the Navier-Stokes problem. This method was introduced by Chorin [10], [11] and Temam [45], [46]. The problem is discretized by the characteristics method in time and the pair $P_1 - P_1$ of finite elements in space which does not satisfy the inf-sup stability condition. To avoid this condition, many stabilizing approaches have been proposed, among which we cite [40].
The algorithm of the projection method is based on the decomposition of the velocity vector field into

a vector of divergence free and another irrotational. Typically, the algorithm is decomposed at each time step into three steps: the first step computes an intermediate velocity that does not satisfy the incompressibility condition; the second step projects this intermediate velocity on the set of divergence free functions to get the value of the pressure solution of the problem; The third step updates the final velocity from the obtained results. The algorithm is summarized as follows : We start with $\mathbf{u}_h^0 = \mathbf{0}$ and $p_h^0 = 0$. Given $\mathbf{u}^n$, find $(\mathbf{u}^{n+1}, p^{n+1})$ such that :

Step1- Computation of the intermediate velocity $\mathbf{u}^*$:

$$\begin{cases} \rho(x)\dfrac{\mathbf{u}^* - \mathbf{u}^n o X^n}{\Delta t} - \operatorname{div}(\mu(x)\nabla\mathbf{u}^*) + \nabla p^n = \rho(x) g\mathbf{e_d} & \text{in} \quad \Omega, \\ [\ \mu(x)\dfrac{\partial \mathbf{u}^*}{\partial \mathbf{n}}\ ] = 0 & \text{in} \quad \Gamma, \\ \mathbf{u}^* = U_{in} & \text{on} \quad \Gamma_0, \\ (BCU) \quad \text{Dirichlet or Navier} & \text{on} \quad \Gamma_1, \\ \mu(x)\dfrac{\partial \mathbf{u}^*}{\partial \mathbf{n}} = 0 & \text{on} \quad \Gamma_2. \end{cases} \tag{5.1}$$

Step 2- Computation of the pressure p^{n+1}:

$$\begin{cases} \operatorname{div}\mathbf{u}^* - \operatorname{div}\Big(\dfrac{\Delta t}{\rho(x)}\nabla(p^{n+1} - p^n)\Big) = 0 & \text{in} \quad \Omega, \\ [\ p^{n+1} - p^n\ ] = 0 & \text{on} \quad \Gamma, \\ \dfrac{\partial}{\partial \mathbf{n}}(p^{n+1} - p^n) = 0 & \text{on} \quad \Gamma_0 \cup \Gamma_1, \\ p^{n+1} - p^n = 0 & \text{on} \quad \Gamma_2. \end{cases} \tag{5.2}$$

Step 3- Computation of the final velocity $\mathbf{u}^{n+1}$:

- For Dirichlet boundary condition:

$$\mathbf{u}^{n+1} = \mathbf{u}^* - \frac{\Delta t}{\rho(x)}\nabla(p^{n+1} - p^n) \quad \text{in} \quad \Omega. \tag{5.3}$$

- For Navier boundary conditions, we solve the following problem:

$$\begin{cases} -\varepsilon'\Delta\mathbf{u}^{n+1} + \mathbf{u}^{n+1} = \mathbf{u}^* - \dfrac{\Delta t}{\rho(x)}\nabla(p^{n+1} - p^n) & \text{in} \quad \Omega. \\ \mathbf{u}^{n+1} = U_{in} & \text{on} \quad \Gamma_0, \\ \dfrac{1}{\beta}\ \mathbf{u}^{n+1}.\mathbf{n} + \ {}^t\mathbf{n}(\varepsilon'\nabla\mathbf{u}^{n+1}).\tau = 0 & \text{on} \quad \Gamma_1, \\ \dfrac{\partial \mathbf{u}^{n+1}}{\partial \mathbf{n}} = 0 & \text{on} \quad \Gamma_2, \end{cases} \tag{5.4}$$

  where ε' is the parameter of penalization which is a small number.

The computed pressure is in $M = \{q \in H^1(\Omega)/q|_{\Gamma_2} = 0\}$ and not in $L_0^2(\Omega)$ and the final velocity belongs to the space $H^0_{\text{div}}(\Omega) = \{\mathbf{v} \in L^2(\Omega)/\operatorname{div}\mathbf{v} = 0 \text{ in } \Omega\}$ in the case of Dirichlet boundary conditions and in $H^1(\Omega)$ in the case of the Navier boundary conditions.(see Bell and Marcus [7]).
For the discretization in space, we introduce the following discrete spaces:

$$\begin{aligned} X_{uh} &= \{\mathbf{u}_h \in X_{\mathbf{u}}; \forall k \in \tau_h; \mathbf{u}_{h|k} \in P_1(k)^d\}, \\ X_{vh} &= \{\mathbf{v}_h \in X_{\mathbf{v}}; \forall k \in \tau_h; \mathbf{v}_{h|k} \in P_1(k)^d\}, \\ M_h &= \{q_h \in M \cap C^0(\Omega); \forall k \in \tau_h, q_{h|k} \in P_1(k)\} \\ L_h &= \{\mathbf{u}_h \in L^2(\Omega); \forall k \in \tau_h; \mathbf{u}_{h|k} \in P_1(k)^d\}. \end{aligned}$$

The discrete variational formulation can be written in the following form:

1- Find $\mathbf{u}_h^* \in X_{uh}$ such that for all $\mathbf{v}_h \in X_{vh}$, we have:

- For Dirichlet boundary condition:

$$\int_\Omega \rho(x)\frac{\mathbf{u}_h^* - \mathbf{u}_h^n o X^n}{\Delta t}\mathbf{v}_h + \int_\Omega \mu(x)\nabla\mathbf{u}_h^*\nabla\mathbf{v}_h + \int_\Omega \nabla p^n \mathbf{v}_h = \int_\Omega \rho(x) g\mathbf{e_d}\mathbf{v}_h. \tag{5.5}$$

- For Navier boundary condition:

$$\begin{aligned}&\int_\Omega \rho(x)\frac{\mathbf{u}_h^* - \mathbf{u}_h^n o X^n}{\Delta t}\mathbf{v}_h + \int_\Omega \mu(x)\nabla\mathbf{u}_h^*\nabla\mathbf{v}_h + \int_\Omega \nabla p^n\mathbf{v}_h \\ &-\int_{\Gamma_1} \alpha\ {}^t\mathbf{u}_h^{n+1}(\boldsymbol{\tau}\ \ {}^t\boldsymbol{\tau})\mathbf{v}_h ds - \int_{\Gamma_1}\beta^{-1}\ {}^t\mathbf{u}_h^{n+1}(\mathbf{n}\ \ {}^t\mathbf{n})\mathbf{v}_h ds = \int_\Omega \rho(x) g\mathbf{e_d}\mathbf{v}_h.\end{aligned} \tag{5.6}$$

2- Find $p_h^{n+1} \in M_h$ such that for all $q_h \in M_h$, we have:

$$\int_\Omega \operatorname{div}\mathbf{u}_\mathbf{h}^* q_h + \int_\Omega \frac{\Delta t}{\rho(x)}\nabla(p_h^{n+1} - p_h^n)\nabla q_h = 0. \tag{5.7}$$

3- Find $\mathbf{u}_h^{n+1}$ such that,

- For Dirichlet boundary condition:
  Find $\mathbf{u}_h^{n+1} \in L_h$ such that for all $\mathbf{v}_h \in L_h$, we have:

$$\int_\Omega \mathbf{u}_h^{n+1}\mathbf{v}_h = \int_\Omega \mathbf{u}_h^*\mathbf{v}_h - \int_\Omega \frac{\Delta t}{\rho(x)}\nabla(p_h^{n+1} - p_h^n)\mathbf{v}_h. \tag{5.8}$$

- For Navier boundary condition:
  Find $\mathbf{u}_h^{n+1} \in X_{uh}$ such that for all $\mathbf{v}_h \in X_{vh}$, we have:

$$\int_\Omega \varepsilon'\nabla\mathbf{u}_h^{n+1}\nabla\mathbf{v}_h - \int_{\Gamma_1}\beta^{-1}\ {}^t\mathbf{u}_h^{n+1}(\mathbf{n}\ \ {}^t\mathbf{n})\mathbf{v}_h ds + \int_\Omega \mathbf{u}_h^{n+1}\mathbf{v}_h = \int_\Omega \mathbf{u}_h^*\mathbf{v}_h - \int_\Omega \frac{\Delta t}{\rho(x)}\nabla(p_h^{n+1} - p_h^n)\mathbf{v}_h. \tag{5.9}$$

6. Level set correction

It is well known that numerous errors affect the numerical algorithm and perturb the mass conservation as time evolves in two phase flow modeling. In this section, we introduce several corrections and ameliorations of the algorithm in order to get satisfying results.

6.1. **Algorithm of reinitialization.**

At the initial time, all levels lines are calculated using the definition of the Level-Set method. As time evolves, the advection of the Level-Set by a velocity field causes the contour lines to become very tight (steep Level-Set) in some areas and spaced (flat Level-Set) in others, thus the method becomes imprecise and algebraic distance property $\|\nabla\phi\| = 1$ is lost. This may cause numerical errors that affect interface shape, its geometric characteristics and, moreover, the mass conservation.

To overcome this, we use the algorithm of reinitialization proposed by Sussman et al. [42] which is based on the following equation

$$\frac{\partial\Phi}{\partial\tau} = sign(\phi)(1 - \|\nabla\Phi\|) \qquad \text{in } \Omega\times(0,\tau), \tag{6.1}$$

with

$$\Phi(x,t,\tau=0) = \phi(x,t), \tag{6.2}$$

where τ is an imaginary time. We solve (6.1) iteratively until it reaches a steady state, we obtain the distance property $||\nabla\Phi|| = 1$.

In order to discreticize the equation (6.1), we rewrite it in the following form:

$$\frac{\partial\Phi}{\partial\tau} + w\nabla\Phi = sign(\phi) \ \text{ with } w = sign(\phi)\frac{\nabla\Phi}{\|\nabla\Phi\|}, \tag{6.3}$$

where $\Delta\tau$ is the time step corresponding to the imaginary time τ.
By using the characteristics method, the discrete variational formulation can be written as:

$$\begin{array}{l}\text{Find } \Phi^{n+1} \in Y \text{ such that } \forall r \in Y,\\ \Big(\dfrac{\Phi^{n+1} - \Phi^n oX^n_{(\mathbf{w}^n,\Delta\tau)}}{\Delta\tau}, r\Big) - (sign(\phi)^n, r) = 0.\end{array} \tag{6.4}$$

The space discretization follows exactly the space discretization of the Level-Set transport equation. The function $sign(\phi)^n$, is approximated numerically by a smoothed function. This smoothness is important to obtain better properties of conservation and to insure stability (See [32]):

$$sign(\phi)^n_h = \frac{\phi^n_h}{\sqrt{(\phi^n_h)^2 + h^2\|\nabla\phi^n_h\|^2}}. \tag{6.5}$$

The discrete variational formulation can be written as:

$$\begin{array}{l}\text{Find } \Phi^{n+1}_h \in Y_h \text{ such that } \forall r_h \in Y_h,\\ \Big(\dfrac{\Phi^{n+1}_h - \Phi^n_h oX^n_{(\mathbf{w_h}^n,\Delta\tau)}}{\Delta\tau}, r_h\Big) - (sign(\phi)^n_h, r_h) = 0.\end{array} \tag{6.6}$$

6.2. **Mass conservation.** The resolution of the transport equation of the Level-Set function causes the diffusion of a small amount of mass at each time step. It can be either an increase or a decrease of the error according to the topological changes of the interface. As time evolves these errors will typically accumulate. But the flow we considered is incompressible this implies that the volume occupied by any of the fluids should be preserved as well. There exists in the litterature many approaches that can be used in order to preserve the mass. We may cite for example Chang et al. [9], Sussman and Fatemi [38].

In this paper, we follow the method proposed by Smolianski [41] which seems simple, cheap and very efficient in our case. The simplicity of the method comes from the fact that the mass conservation can be enforced by adding a three lines algorithmic step. The key observation is that the error in mass balance should be very small within one time-step, usually this is done by using a sufficiently accurate scheme for the convection of level-set function. In our case we were be able to reduce the volume error remarkably by using the new proposed boundary condition (as we will see in the numerical results) which makes the computational strategy remarkably cheap and efficient.
The concept of the method is to vary the zero isocontour at each time step by moving the level-set function, i.e. by adding to Φ some signed constant c_Φ, where $|c_\Phi|$ is the distance between the old and new zero-level sets such that the new level-set function Φ_{new} reduces the error of the corresponding mass and defines a new domain

$$\Omega_2^{new} = \{\mathbf{x} \in \Omega : \Phi_{new} > 0\}.$$

The expression of c_Φ is given by the formula

$$\begin{aligned} S_{exact} - S(\Omega_2) &= \int_{\Omega_2^{new}} dx - \int_{\Omega_2} dx \\ &= \int_\Gamma (c_\Phi \mathbf{n}).\mathbf{n} d\Gamma + O(c_\Phi^2) \\ &= c_\Phi \int_\Gamma d\Gamma + O(c_\Phi^2), \end{aligned} \tag{6.7}$$

where S_{exact} is the exact area (or volume in 3D) of the region occupied by the second fluid, $S(\Omega_2)$ is the numerical area of Ω_2 . By denoting $L = \displaystyle\int_\Gamma d\Gamma$, we approximate c_Φ by

$$c_\Phi \simeq \frac{S_{exact} - S(\Omega_2)}{L(\Gamma)}. \tag{6.8}$$

Then the corrected level set function becomes

$$\Phi_{new} \simeq \Phi + c_\Phi ||\nabla\Phi||. \tag{6.9}$$

The formula (6.8) is accurate up to $O(c_\Phi^2)$. First, it is noteworthy that if $S(\Omega_2) > S_{exact}$, we have $c_\Phi < 0$ and the level-set function Φ will be moved downward. if $S(\Omega_2) < S_{exact}$, we have $c_\Phi > 0$ and the level-set function Φ will be moved upward.

Remark 6.1. *By using the reinitialization algorithm which gives* $\| \nabla\Phi \| = 1$*, we can approximate* Φ_{new} *by* $\Phi_{new} = \Phi + c_\Phi$*. But numerically, we have numerical errors and we never reach the relation* $\| \nabla\Phi \| = 1$ *and it is better to use the previous expression (6.9).*

7. Numerical results

In this section, we perform several numerical simulations using the **FreeFem ++** software [23].

7.1. **First test case (2D).** In this case, we consider the time interval $[0, T]$ where $T = 10$ and the initial domain

$$\Omega \cup \Gamma =]0, a[\times]0, b[\ \cup\ ]c, c+d[\times]-e, 0]$$

which is composed of a two-dimensional rectangular tank where $a = 2, b = 1$, $d = 0.4$ and $e = 0.2$. We suppose that this mould contains a small amount of fluid defined by the $\Gamma = [c, c+d]$ (as shown in the figure (2)). The boundary of Ω is decomposed as $\partial\Omega = \Gamma \cup \Gamma_0 \cup \Gamma_1 \cup \Gamma_2$ where

$$\Gamma_0 = [c, c+d] \times \{0\}\ ,\ \Gamma_1 = [0, c] \times \{0\} \cup \{c, c+d\} \times [-e, 0] \cup \{0, a\} \times [0, b] \ \text{ and } \ \Gamma_2 = [0, a] \times \{b\},$$

as shown in the figure below.

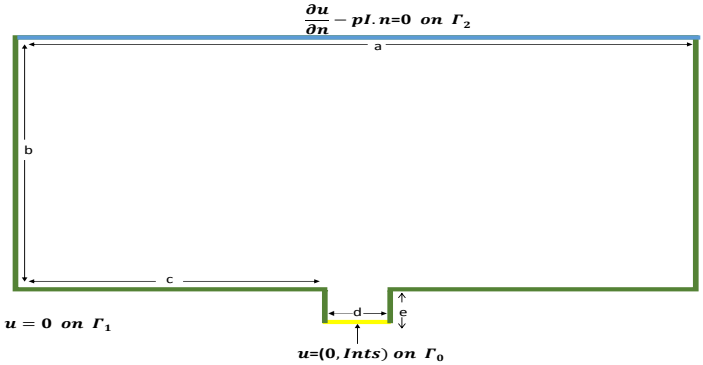

Figure 2. The 2D mould .

The considered mesh contains 7329 vertices and 14316 triangles where the boundaries Γ_0, Γ_1 and Γ_2 are divided into N segments per unit length (where $N = 50$).

At the initial time, the interface Γ is represented by the Level-Set function of equation $\phi_0 = y - 0.1$

Figure 3. The interface at the initial time

For the numerical investigations, we consider the non-dimensionalized incompressible Navier stokes equation:

$$\rho\Big(\frac{\partial \mathbf{u}}{\partial t} + \mathbf{u}.\nabla\mathbf{u}\Big) - \frac{1}{Re}\mu\ \Delta\mathbf{u} + \nabla p = -\rho_1 \frac{1}{Fr^2}\mathbf{e_d}, \tag{7.1}$$

where $Re = \rho_{ref} u_{ref} l_{ref}/\mu_{ref}$ is the Reynolds number, $Fr = u_{ref}/\sqrt{l_{ref} g}$ the Froude number. ρ_{ref} is the density of the first fluid ρ_1, μ_{ref} is the viscosity of the first fluid μ_1, l_{ref} is the diameter of the inlet and u_{ref} is the average velocity of the fluid.
We choose $\rho_{ref} = 10^3 Kg/m^3$, $\mu_{ref} = 10^{-1} Ns/m^2$, $l_{ref} = 0.4m$, $u_{ref} = 0.5m/s$, $\mu_1 = 1$, $\mu_2 = 1$, $\rho_1 = 1$, $\rho_2 = 0.001$, $g = 9.8m/s^2$. Furthermore, we take $U_{in} = 0.5$, $h = \frac{1}{N}$, $\Delta t = 2h$, $\Delta\tau = \Delta t/10$ and $\varepsilon = h/3$.
For the Navier boundary conditions, we consider $\alpha = 0$ and $\beta = 1e-6$ which allow slip without friction.
For the numerical tests, we consider four cases:

- Case *i*: Solution in the sense of viscosity with boundary condition of Dirichlet type for the velocity and homogeneous Neumann type for the Level-Set function before mass conservation.
- Case *ii*: Solution in the sense of viscosity with boundary condition of Navier type for the velocity and homogeneous Neumann type for the Level-Set function before mass conservation.
- Case *iii*: Solution in the sense of viscosity with boundary condition of Navier type for the velocity and non-homogeneous Neumann type for the Level-Set function before mass conservation.
- Case *iv*: Solution in the sense of viscosity with boundary condition of Navier type for the velocity and non-homogeneous Neumann type for the Level-Set function after mass conservation.

Figures (4), (5) and (6) show a comparison of the numerical results for the 4 considered cases at $t = 1$, $t = 5$ and $t = 9$.

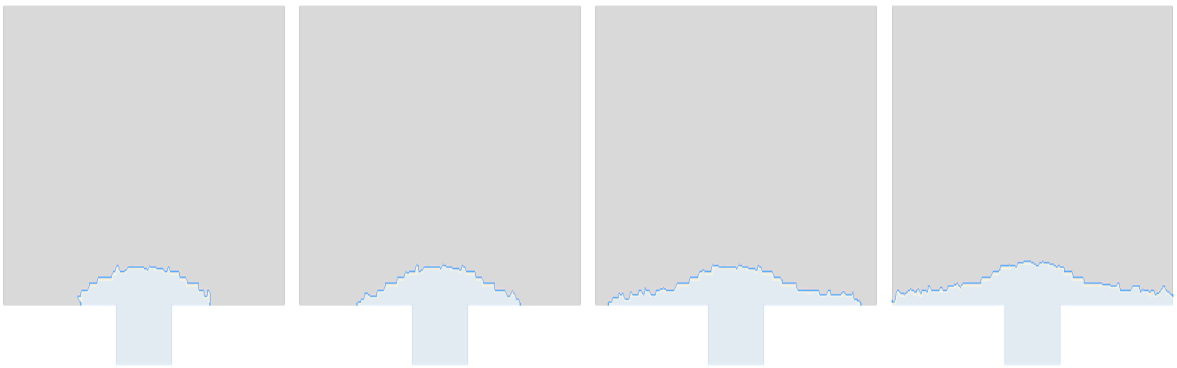

FIGURE 4. At t=1, From left to right: case i, case ii, case iii, case iv

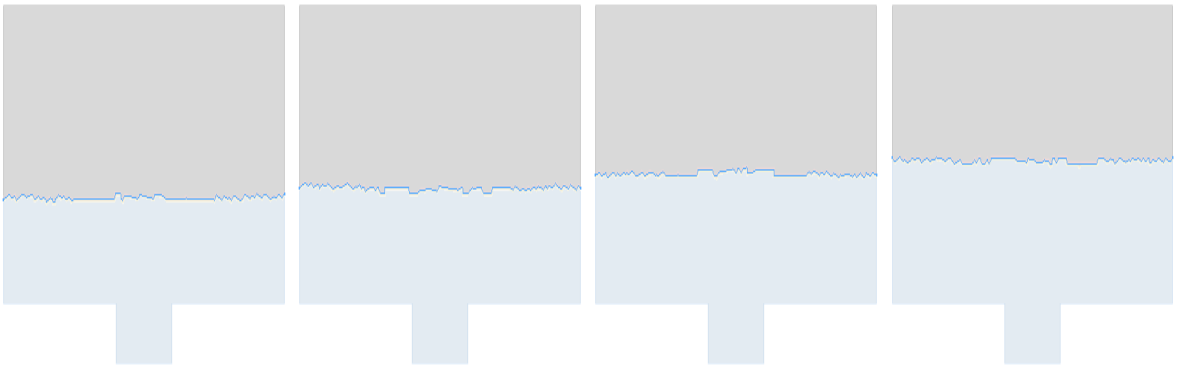

FIGURE 5. At t=5, From left to right: case i, case ii, case iii, case iv

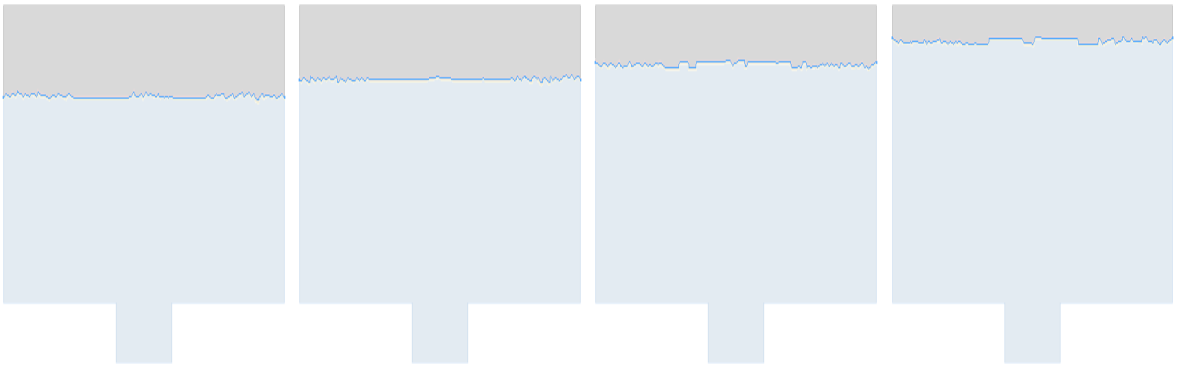

FIGURE 6. At t=9, From left to right: case i, case ii, case iii, case iv

Figures (4), (5) and (6) show that in case i, boundary layers phenomena appear between the free surface and the wall boundaries, which are corrected in case ii by using Navier-Boundary conditions. We still have a non-physical phenomenon concerning the right angle showed between the free surface and the wall boundaries. In the case iii, we impose natural boundary conditions under pressure effect that gives a natural angle between the free surface and the wall boundaries. We notice an increase of the volume of fluids among the cases which will be justified later. In case iv, we show numerical results after the mass conservation correction step.

To validate the effectiveness of the proposed scheme in the case of the non-homogeneous Neumann boundary condition under pressure effect for the Level-Set function, we analyze the error of the volume evolving in time:

$$err_V = \frac{|V_e - V_n|}{|V_n|},$$

where V_e is the exact volume and V_n is the numerical volume.
Figure (7) shows a comparison between the volume error by using the classical method and the projection method for $\varepsilon = h/3$.

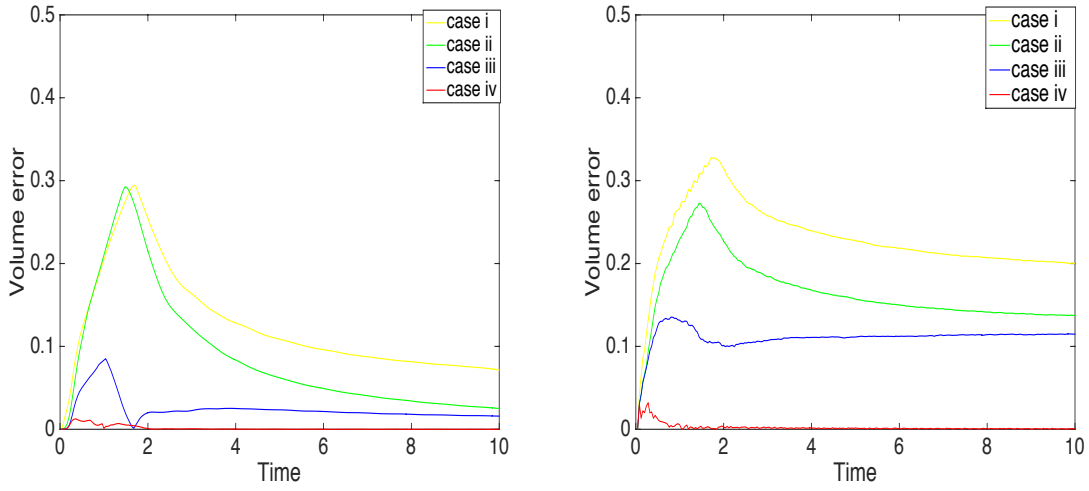

FIGURE 7. Comparison of the volume error for the cases i, ii, iii and iv for $\varepsilon = h/3$. To the left: classical method; To the right projection method

We deduce that the classical method and the projection method give very close results. The volume error in the classical method is better than that in the projection method. However, the CPU time and memory in the projection method are remarkably lower. Thus we will continue our work in 3D using the projection method. As for the comparison between the 4 considered cases, we may infer that the volume error reaches more than 35% in the case i, it decreases in the case ii with Navier boundary condition with allows the fluid to slip, it decreases remarkably in the case iii with the new proposed boundary condition under pressure effect. And because the error became small enough at each time step, we were able to apply the mentioned mass conservation algorithm in the case iv where the volume error reaches a maximum of 3% in the beginning and it decreases to less than 0.5% in the rest of the computational process.
Figure (8) shows the error err_V with respect to the time iteration for the case iv. It decreases with the space step (when N increases) which implies the convergence of the method.

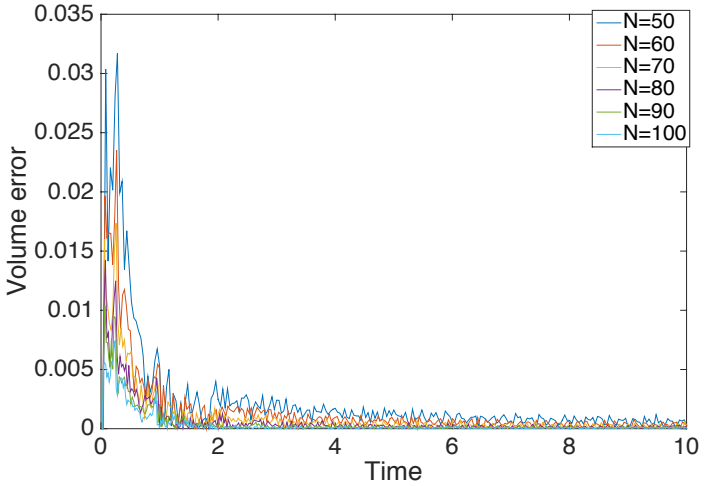

FIGURE 8. Comparison of the volume error for N varying from 50 till 100 in the case iv.

7.2. **Second test case (3D).** In this section, we consider the same data of the previous section but with a 3D case and $N = 50$, the considered mesh contains 180816 vertices and 1111810 tetrahedrons. The domain Ω is a parallelepiped, with a rectangular base whose dimensions are $a = 1, b = 1$ and of height $z = 1$ centred with a small hole in the bottom face whose dimensions are $a_1 = b_1 = 0.4, e = .12$ (see figure 9 to the left). In 3 dimensional problems, we consider the regularity parameter to be $\varepsilon = h/3$.

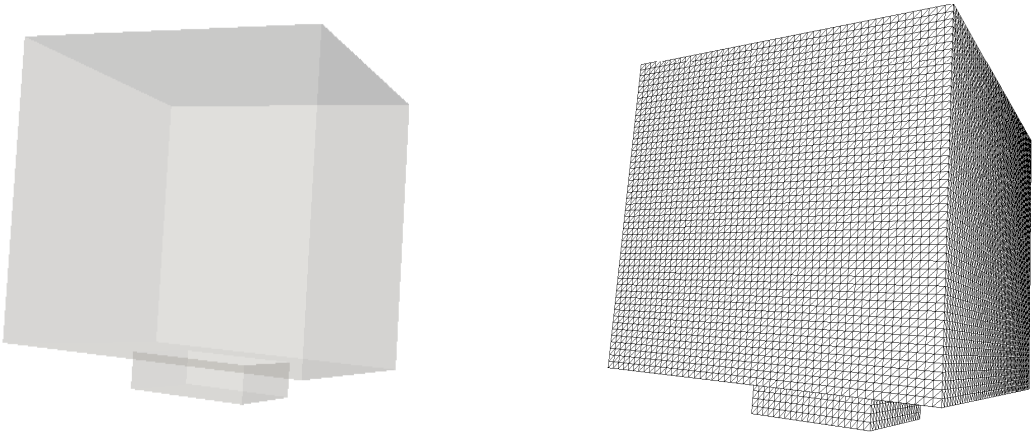

FIGURE 9. To the left: The cube mould. To the right : The cube mesh.

At the initial time, the interface Γ is represented by the Level-Set function of equation $\phi_0 = z - 0.06$ Figures 10-11 show the evolution of interface at the initial time, $t = 0.4$, $t = 1$, $t = 4$, $t = 6$, and $t = 8$.

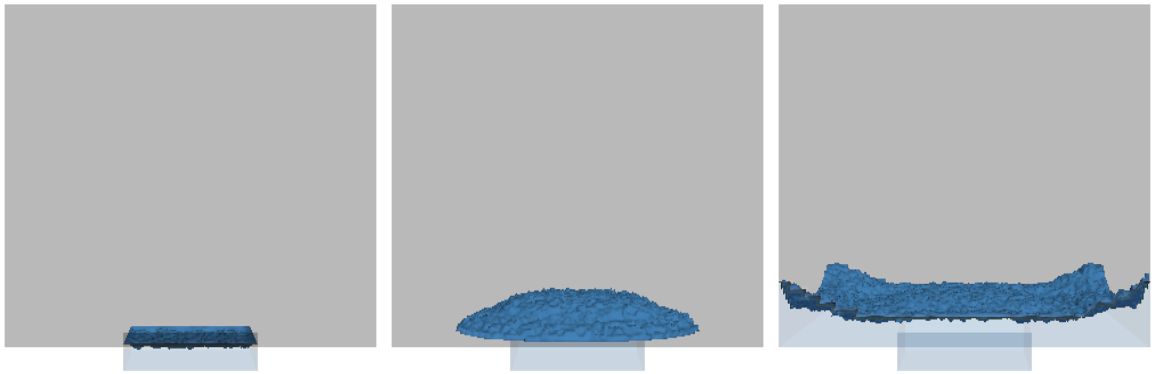

FIGURE 10. The approximated interface at $t = 0$, $t = 0.4$ and $t = 1$.

FIGURE 11. The approximated interface at $t = 4$, $t = 6$ and $t = 8$.

Figure (12) shows the evolution of the error err_V during time for the cases i, ii, iii and iv.

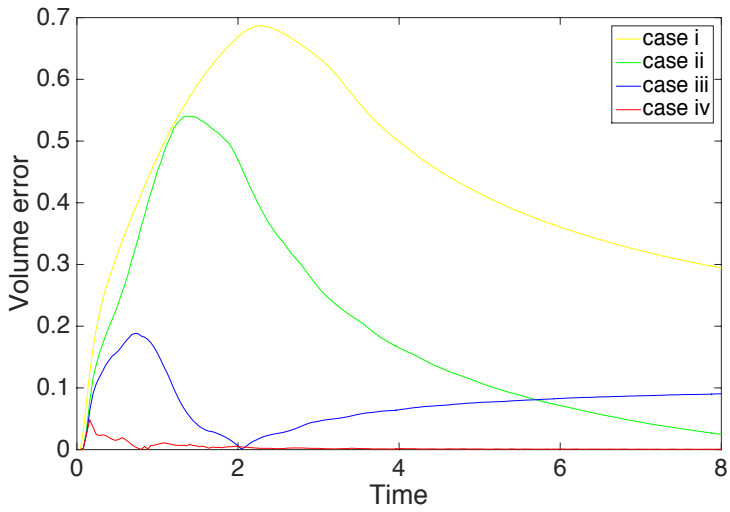

FIGURE 12. The relative volume error for the second test case (in 3D).

One more time, the graph of the volume error in figure (12) shows the efficiency of the algorithm in 3 dimensional problems.

7.3. **Industrial case.** In this section, we model mould filling. The domain Ω is a mould as it is shown in the figure (13). We intend here to fill the mould and to study the interface transport that separates the two fluids.

Thus we consider $\rho_{ref} = 7 * 10^3 Kg/m^3$, $\mu_{ref} = 0.01 Ns/m^2$, $l_{ref} = 0.045m$, $u_{ref} = 0.2m/s$, $\mu_1 = 1$, $\mu_2 = 1$, $\rho_1 = 1$, $\rho_2 = 0.001/7$, $g = 9.8m/s^2$.

Furthermore, we take $U_{in} = 0.2$, $h = \dfrac{1}{N}$, $\Delta t = 2h$, $\Delta\tau = \Delta t/20$ and $\varepsilon = h/3$.

The considered mesh contains 59364 vertices and 294544 tetrahedrons.

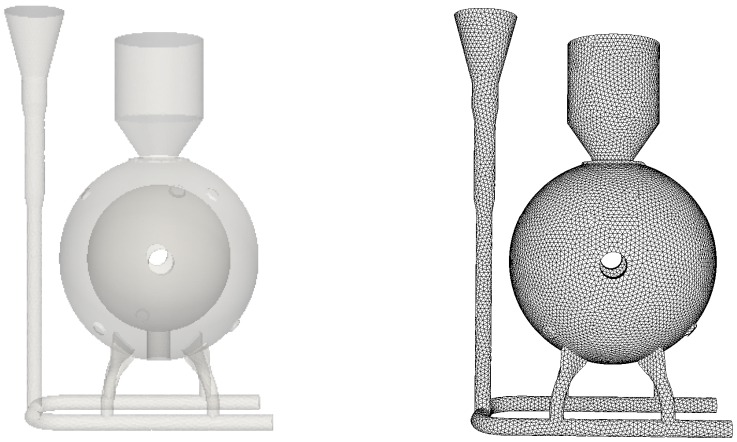

FIGURE 13. To the left: The mould shape; To the right: the mould mesh.

At the initial time, the interface Γ is represented by the Level-Set function of equation $\phi_0 = -z + 0.9$.

Figures 14, 15 and 16 show the evolution of the interface at the initial time, $t = 0.8$, $t = 1.6$, $t = 3.2$, $t = 4.8$, $t = 9.6$, $t = 18$, $t = 20$ and $t = 22$.

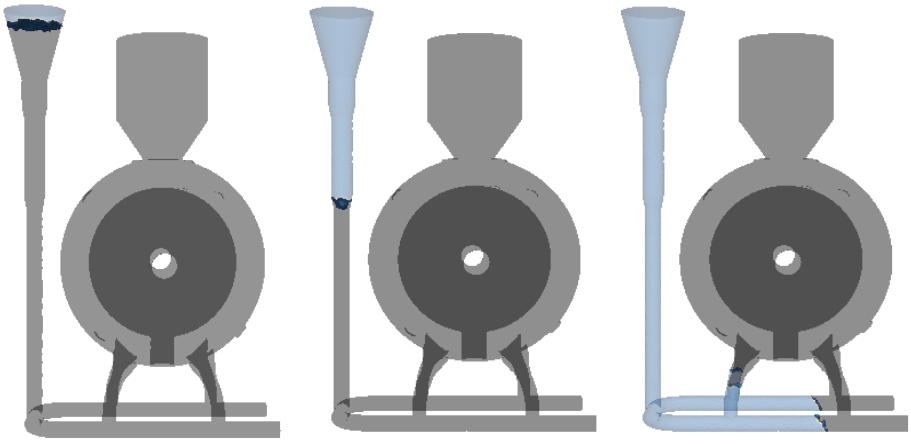

FIGURE 14. The approximated interface at the initial time, $t = 0.8$ and $t = 1.6$.

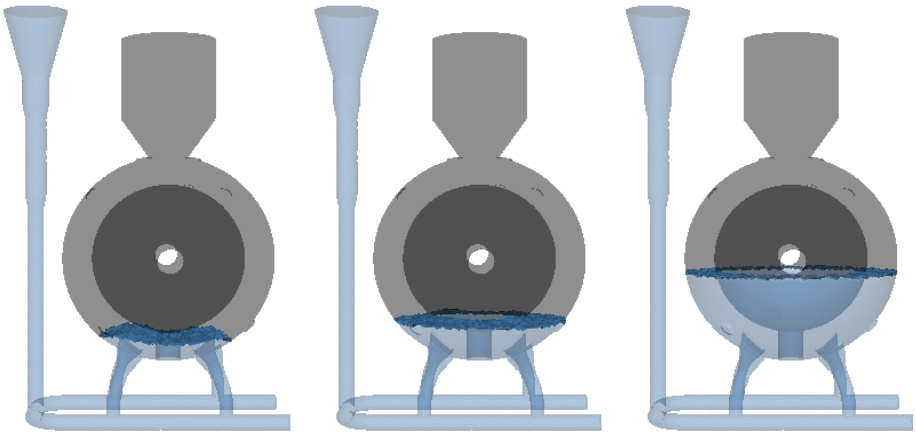

FIGURE 15. The approximated interface at $t = 3.2$, $t = 4.8$ and $t = 9.6$.

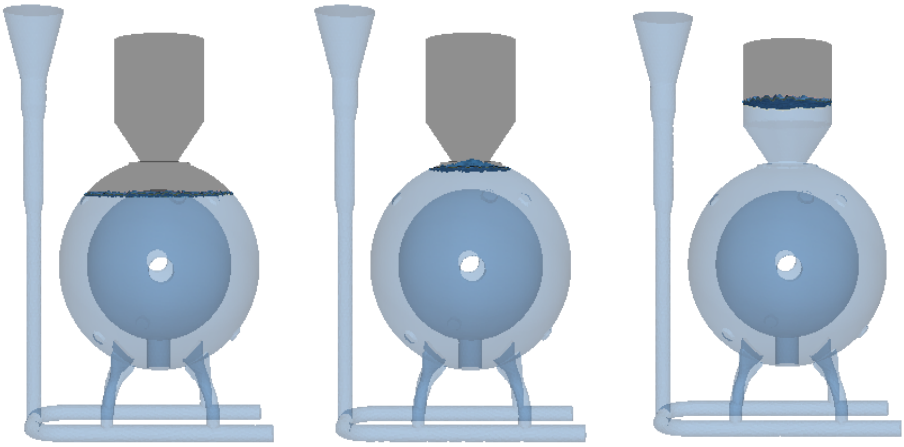

FIGURE 16. The approximated interface at $t = 18$, $t = 20$ and $t = 22$.

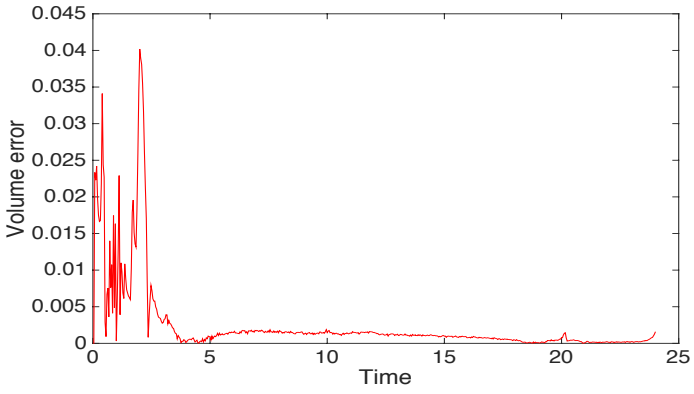

FIGURE 17. Volume error with respect to time in case *iv* for the practical case.

Figure (17) show the evolution of the error during the time for the case *iv*.

One more time, the figure (17) show the efficiency of the algorithm even for practical cases.

8. Conclusion and Perspectives

In this paper, we formulated a computational strategy that models the interface transport scheme in the case of filling a mould. The model consists of coupled nonlinear PDEs for the displacement, the pressure and the Level-Set unknowns. Numerical tests demonstrate the efficiency of the model. Specifically, this approach can treat interface transport of two incompressible immiscible fluids, of high density ratio. In the next paper, in order to reduce the cost of the simulation, we intend to solve the problem using an iterative parallel solver that suits the characteristics method.

References

[1] Anderson D.M., McFadden G.B., Wheeler A.A., Diffuse-interface methods in fluid mechanics, *Annu. Rev. Fluid Mech., 1998; 30: 139-165.*

[2] Babuska I., The Finite Element Method with Penalty , *Mathematics of computation, Volume 27, Number 122, April 1973.*

[3] Baensch E. , Finite element discretization of the Navier-Stokes equations with a free capillary surface, *Numer. Math., 88:203-235, 2001.*

[4] Batchelor G.K. , An Introduction to Fluid Dynamics, *Cambridge University Press, 1967.*

[5] Barles G., Solutions de viscosité et équations elliptiques du deuxième ordre , *Cours, Université de tours, 1997.*

[6] Behr M., Stabilized space-time finite element formulations for free-surface flows., *Comm. Numer. Meth. Engrg., 11:813-819, 2001.*

[7] Bell J.B. and Marcus D.L., A second-order projection method for variable-density flows , *J. Comput. Phys. 101 (1992) 334-348.*

[8] Benqué J.P., Ibler B., Keramsi A., Labadie G., A finite element method for the Navier- Stokes equations, Proceedings of the third international conference on finite elements in flow problems , *Banff. Alberta, Canada 10-13 June (1980).*

[9] Chang Y.C., Hou T.Y., Merriman B. and Osher S., A level set formulation of Eulerian interface capturing methods for incompressible fluid flows, *J. Comput. Phys. 124 (1996) 449-464*

[10] Chorin A.J., Numerical solution of the Navier-Stokes equations, *Math. Comp. 22 (1968) 745-762 .*

[11] Chorin A.J., On the convergence of discrete approximations to the Navier- Stokes equations, *Math. Comp. 23 (1969) 341-353 .*

[12] Crandall M. G. and Lions P. L., Viscosity solutions of Hamilton-Jacobi equations , *Trans. Amer. Math. Soc. 277 (1983), 1-42.*

[13] Cuvelier C., Schulkes R.M., Some numerical methods for the computation of capillary free boundaries governed by the Navier-Stokes equations, *D. Reidel Publishing Company, Dordrecht, 1986.*

[14] Dervieux A., Thomasset F., A finite element method for the simulation of a Rayleigh-Taylor instablity, in Approximation Methods for Navier-Stokes problems, *Lecture Notes in Mathematics, 1980; 771, Springer- Verlag, Berlin, 145-158.*

[15] Donea J., Huerta A. , Finite Element Methods for Flow Problem, *Wiley, 2003.*

[16] G. Fourestey., Stabilité des méthodes de Lagrange-Galerkin du premier et du second ordre , *Technical Report 4505, INRIA Rocquencourt, 2002.*

[17] Gallagher R.H., Carey G.F., Oden J.T., Zienkiewicz O.C., Finite Elements in Fluids , *Vol. 6, J. Wiley and sons, 1985.*

[18] Ganesan S. and Tobiska L., A coupled arbitrary Lagrangian-Eulerian and Lagrangian method for computation of free surface flows with insoluble surfactants, *J. Comp. Phys., 228:2859-2873, 2009.*

[19] Gerlach D., Tomar G., Biswas G., and Durst G., Comparison of volume-of-fluid methods for surface tension-dominant two-phase flows, *International Journal of Heat and MassTransfer, 49:740-754, 2006.*

[20] Esmaeeli A. and Tryggvason G., Direct numerical simulations of bubbly flows. Part 1. Low Reynolds number arrays. , *Journal of Fluid Mechanics, 377:313-345, 1998.*

[21] Esmaeeli A. and Tryggvason G., Direct numerical simulations of bubbly flows. Part 2. Moderate Reynolds number arrays., *Journal of Fluid Mechanics, 385:325-358, 1999.*

[22] Harlow F.H., Welch J.E., Numerical calculation of time-dependent viscous incompressible flow of fluid with free surface, *Phys. Fluids, 1965; 8: 2182-2189.*

[23] Hecht F., New development in FreeFem++, *J. Numer. Math. 20 (2012), no. 3-4, 251-265. 65Y15.*

[24] Hirt C.W., Amsden A.A., and Cook J.L., An arbitrary Lagrangian-Eulerian computing method for all flow speeds., *Journal of Computational Physics, 135:203-216, 1997.*

[25] Hirt C.W. and Nichols B.D., Volume of fluid (VOF) method for the dynamics of free boundaries., *Journal of Computational Physics, 39:201-225, 1981.*

[26] Lamb H., Hydrodynamics., *Cambridge University Press, 1932.*

[27] K.W. Morton, A. Priestley, and E. Suli, Stability of the Lagrange-Galerkin method with non-exact integration, *RAIRO-Modélisation mathématique et analyse numérique, 22(4):625-653, 1988.*
[28] Navier C.L.M.H., Sur les lois de l'équilibre et du mouvement des corps élastiques, *Mem. Acad. R. Sci. Inst. Vol. 6, France (1827) 369.*
[29] Olsson E., Kreiss G., A conservative level set method for two phase flow, *J.Comp. Phys 210 (2005) 225-246.*
[30] Olsson E., Kreiss G., A conservative level set method for two phase flow II, *J.Comp. Phys 225 (2007) 785-807.*
[31] Osher S. and Sethian J.A., Fronts propagating with curvature-dependent speed: algorithms based on Hamilton-Jacobi formulations, *Journal of Computational Physics, 79, pp. 12- 49, 1988.*
[32] Peng D., Merriman B., Osher S., Zhao H., and Kang M., A PDE-based fast local level set method, *Journal of Computational Physics, 155, pp. 410-438, 1999.*
[33] Pironneau O., On the transport-diffusion algorithm and its applications to the Navier-Stokes equations , *38(3):309-332, 1982.*
[34] Qian T., Wang X.P. and Sheng P., Molecular Hydrodynamics of the Moving Contact Line in Two-phase Immiscible Flows , *COMMUNICATIONS IN COMPUTATIONAL PHYSICS Vol. 1, No. 1, pp. 1-52, February 2006.*
[35] Scardovelli R. and Zaleski S., Direct numerical simulation of free-surface and interfacial flow. , *Ann. Rev. Fluid Mech., 31:567-603, 1999.*
[36] Serrin J., Mathematical principles of classical fluid mechanics, *Handbuch der Physik, pp. 125-263, Springer- Verlag, 1959.*
[37] Shin S., Juric D., Modeling three-dimensional multiphase flow using a level contour reconstruction method for front tracking without connectivity, *J. Comput. Phys., 2002; 180: 427-470.*
[38] M. Sussman and E. Fatemi, An efficient interface-preserving level set redistancing algorithm and its application to interfacial incompressible fluid flow, *SIAM J. Sci. Comput. 20 (1999), no. 4, 1165-1191.*
[39] Shyy W., Udaykumar H.S., Rao M.M., Smith R.W., Computational Fluid Dynamics with moving Boundaries,, *Taylor and Francis, 1996.*
[40] Shen J., On a new pseudocompressibility methods for the incompressible Navier-Stokes equations , *Appl. Numer. Math. Vol 21, pp. 71-90,1996 .*
[41] A. Smalonski , Numerical Modeling of Two-Fluid Interfacial Flows , *PhD thesis University of Jyvaskyla Finland 2001.*
[42] Sussman M., Smereka P., Osher S., A level set approach for computing solutions to incompressible two-phase flows, *J. Comput. Phys., 1994; 114: 146-159.*
[43] Sussman M., Almgren A., Bell J., Colella Ph., Howell L. and Welcome M., An adaptive level set approach for incompressible two-phase flows, *J. Comput. Phys. 148 (1999) 81-124.*
[44] Tanaka N., Global existence of two-phase non-homogeneous viscous incompressible fluid flow , *Comm. in Partial Differential Equations, 18:41-81, 1993.*
[45] Temam R., Sur l'approximation de la solution des équations de Navier- Stokes par la méthode des pas fractionnaires (I), *Arch. Rational Mech. Anal. 32 (1969) 135-153.*
[46] Temam R., Sur l'approximation de la solution des équations de Navier- Stokes par la méthode des pas fractionnaires (II) , *Arch. Rational Mech. Anal. 33 (1969) 377-385.*
[47] Tome M.F., Castelo A., Cuminato J.A., Mangiavacchi N., and McKee S., a numerical method for solving unsteady three-dimensional free surface flows., *Journal of Computational Physics, 157:441-472, 2000.*
[48] Torres D.J., Brackbill J.U., The point-set method: front-tracking without connectivity, *J. Comput. Phys., 2000; 165: 620-644.*
[49] Unverdi S.O. and Tryggvason G., A front-tracking method for viscous incompressible multi-fluid flows. , *Journal of Computational Physics, 100:25-37, 1992.*
[50] Zhang H., Zheng L.L., Prasad V. and Hou T.Y., A curvilinear level set formulation for highly deformable free surface problems with application to solidication, *Numer. Heat Transfer, part B, 34 (1998), 120.*
[51] Zhao H.K., Merriman B., Osher S. and Wang L., Capturing the behavior of bubbles and drops using the variational level set approach, *J. Comput. Phys. 143 (1998) 495-518.*